MDPI

Article

Suppressing Polarization Mode Dispersion with the Quantum Zeno Effect

Ian Nodurft [1,2,†], Alejandro Rodriguez Perez [2], Naveed Naimipour [2], and Harry Shaw [2,*]

[1] Peraton; inodurft@peraton.com
[2] NASA Goddard Space Flight Center; ian.c.nodurft@nasa.gov
* Correspondence: harry.c.shaw@nasa.gov;
† Current address: Affiliation.

Abstract: Polarization mode dispersion can introduce quantum decoherence in polarization encoded information, limiting the range of quantum communications protocols. Therefore, strategies to completely nullify the affect would reduce quantum decoherence and potentially increase the operational range of such technology. We construct a quantum model of polarization mode dispersion alongside a two-level absorbing material. The two-level material serves to destructively measure one of two orthogonal polarization modes, thus projecting the polarization onto the other state. The theoretical results are supported by a numerical simulation in Mathematica Documentation where we and compare the evolution of the polarization state with and without the absorbing material. We find that this strategy is effective in suppressing the effects of polarization mode dispersion, and that this method produces a global phase shift related the waveguide's birefringent properties.

Keywords: Zeno; Polarization Mode Dispersion; polarization; quantum Zeno effect; PMD; optical fibers; fibers; waveguides

Citation: Nodurft, I.; Rodriguez Perez, A.; Shaw, H. Suppressing Polarization Mode Dispersion with the Quantum Zeno Effect. *Journal Not Specified* **2024**, *1*, 0. https://doi.org/

Received:
Revised:
Accepted:
Published:

1. Introduction

Polarization mode dispersion (PMD) is a near unavoidable feature of fiber optical communications, wherein the polarization state of light passing through a medium (optical fibers) shifts and changes as it travels [1]. In fibers, for example, this is the consequence of birefringence present in the optical fiber waveguide due to unintentional variations in the shape of the core [1–4]. Strategies employed to compensate and avoid it include intentionally exaggerating the birefringence such that cross-talk between two orthogonal polarization states is negligible, also known as polarization maintaining fibers (PMF) [1,5–7, 10] among other methods [8,9]. However, various environmental effects (wind, temperature, etc.) can cause the fibers to bend and twist, further randomizing the birefringence and reintroducing PMD into the fiber [11].

PMD can be particularly detrimental to quantum communications as qubits encoded (especially entangled) states in the polarization degree of freedom are susceptible to decoherence or errors as a result, limiting the range of quantum communications relying on such states. Some errors can be avoided or corrected through the use of cluster states [12,13] and error-correcting codes [14], but these of course have their limitations such as scalability issues from large overhead in physical resources required to create them or cannot be reversed.

Our proposed method relies instead on the quantum Zeno effect, the phenomenon in which repeated, frequent measurements (or interactions) prevent a quantum system from evolving [15,16]. Creative use of the Zeno effect can induce unusual phase shifts or turn probabilistic processes into fully deterministic ones and it has been proposed for several such purposes [18–21], and experimentally demonstrated [17].

In our case, the Zeno effect is induced by the introduction of a two-level absorbing medium into the evanescent field of an optical waveguide (fiber). The absorbing medium

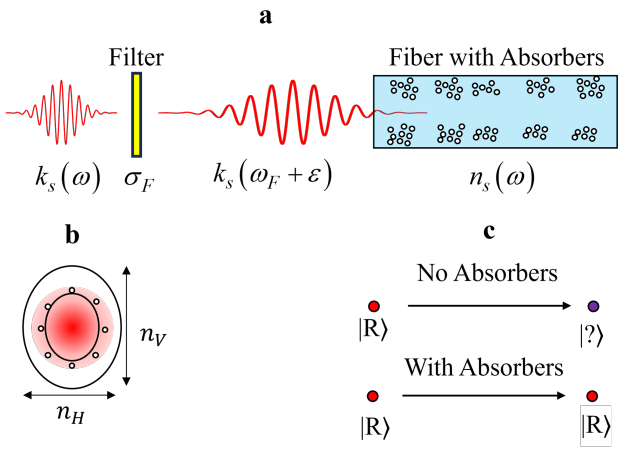

Figure 1. Visual outline of the proposed PMD suppression technique. a) Outline of major assumptions about the physical scenario, with a single photon passing through a narrow bandwidth filter, followed by entering an optical waveguide (fiber) containing an absorbing medium. b) An example cross-section of an optical fiber overlaid with an electromagnetic field, with an elliptical shape rather than the ideal circular shape. This gives the differential refractive index between horizontal and vertical polarizations. c) A simple depiction of the polarization state at the input and output of a fiber with and without the absorbing medium. Without absorbers, the polarization is unknown at the end, whereas the polarization is preserved with the absorbers present.

will be assumed on resonance with a given frequency of either right or left circular polarized photons while the actual photon passing through will be the opposite polarization. Without loss of generality, we will assume throughout this paper that the absorbing medium is resonant with left-circularly polarized photons while the photons travelling through the fiber will be assumed right-circularly polarized. The presence of the absorbing material will serve to destroy any left-circularly polarized photons that appear in the waveguide, while letting right-circular photons through unhindered. The proposed design and its operation are depicted in Figure 1.

By suppressing the effects of birefringence, it may become possible to transmit arbitrary qubits encoded in the polarization degree of freedom without introducing any decoherence.

In section 2, we will construct a theoretical model for PMD acting on a single photon of right-circular polarization, followed by a derivation of the Zeno effect acting on the photon in such an environment. Section 3 will show the results of a numerical simulation corroborating the theoretical predictions and we will conclude in section 4.

2. Theory

We consider the situation depicted in Figure 1. A single photon is injected into an optical fiber after passing through a narrow frequency bandwidth filter. The general single photon state is given by [22,23]

$$|\psi(0)\rangle = c_N \int d\omega g(\omega) \hat{a}^\dagger_{k,s} |0\rangle. \tag{1}$$

The function $g(\omega)$ is determined by the source, but having passed through a narrow bandwidth filter, it can be approximated by a Gaussian distribution centered on frequency ω_F. The constant c_N is a suitable normalization constant, and the subscripts k and s refer to the wavenumber and polarizations respectively. To obtain the time-dependence of the polarization, we apply the positive frequency component of the electric field operator in one dimension [24]

$$\hat{\mathbf{E}}(x,t) = i \sum_{k,s} \sqrt{\frac{2\pi\hbar\omega_k}{V}} \hat{\mathbf{e}}_{k,s} e^{i(kx-\omega_k t)}. \tag{2}$$

Applying Eq. (1) to Eq. (2), and replacing $g(\omega) \to \exp\left[-(\omega-\omega_F)^2/\sigma_F^2\right]$ we obtain the time-dependent state

$$|\psi(t)\rangle = c'_N \int d\omega \sqrt{\omega} e^{\frac{-(\omega-\omega_F)^2}{\sigma_F^2}} e^{-i\omega t}[e^{ik_H x_H}|H\rangle - ie^{ik_V x_V}|V\rangle] \tag{3}$$

where we have further assumed the photon begins in the polarization state $|R\rangle = (|H\rangle - i|V\rangle)/\sqrt{2}$.

Note that the wavenumber is different for the two polarization states, representative of the birefringence which produces polarization mode dispersion. In general, these values will themselves change with time, but we have assumed here constant birefringence. We will leave the majority of the remainder of this derivation for the Appendix A.1, but a few important replacements will be noted here. We first assume constant birefringence, and replace the wavenumber with

$$k_s = k_{0,s} + \alpha_s(\omega - \omega_F) + \beta_s(\omega - \omega_F)^2 \tag{4}$$

and the frequency under the integral is replaced by

$$\omega_k = \omega_F + \epsilon. \tag{5}$$

The narrow bandwidth filter accounts for the factor of $\sqrt{\omega}$ as noted in Appendix A.1 and the integral is taken over all frequencies as an approximation. We also make the replacement $x_s \to v_s t = ct/n_s$ where n_s is the refractive index of an s polarized photon.

Evaluating the integral (3) under these approximations, we obtain

$$|\psi(t)\rangle = c''_N\Big(\frac{e^{\frac{(\alpha_H x_H - t)^2}{4(-\frac{1}{2\sigma_F^2}+i\beta_H x_H)}}}{\sqrt{-\frac{1}{2\sigma_F^2}+i\beta_H x_H}}|H\rangle - i\frac{e^{\frac{(\alpha_V x_V - t)^2}{4(-\frac{1}{2\sigma_F^2}+i\beta_V x_V)}}}{\sqrt{-\frac{1}{2\sigma_F^2}+i\beta_V x_V}}|V\rangle\Big). \tag{6}$$

This general result is reducible to

$$|\psi(t)\rangle \approx \frac{1}{\sqrt{2}}\Big(e^{-i\phi_H t}|H\rangle - ie^{-i\phi_V t}|V\rangle\Big) \tag{7}$$

where

$$\phi_s = \begin{cases} 2\sigma_F^2 c\frac{\beta_s}{n_s}, & t \to 0^+ \\ \frac{n_s}{4\beta_s c}(\frac{\alpha_s}{n_s} - 1)^2, & t \to \infty \end{cases}. \tag{8}$$

An important step in obtaining this result is the replacement $x_s \to v_s t = ct/n_s$. Note that the convenient form of the polarization time-dependence in (7) is valid for time-scales much smaller or larger than $t = n_s/(2\sigma_F^2|\beta_s|c)$ for either polarization s.

A time-evolution operator is easily obtained by inspection from (7),

$$\hat{U}(t) = \begin{bmatrix} e^{-i\phi_H t} & 0 \\ 0 & e^{-i\phi_V t} \end{bmatrix}, \tag{9}$$

from which we can derive the dynamics of the system under continuous observation [16]. Projecting this operator an infinite number of times within a finite time T produces the effective time-evolution operator

$$\hat{V}(T) = e^{\frac{i}{2}(\phi_H+\phi_V)T}|R\rangle\langle R| \tag{10}$$

The full derivation is provided in Appendix A.2. Interestingly, the phase shift of the polarized state under the Zeno effect is equivalent to the average of the horizontal and vertical phase shifts, necessarily those of the short timescale in (8).

The question remains, what conditions are required for the Zeno effect to be successful? In general, the physical situation in which the Zeno effect arises is any of those cases where the transition into some undesired state (in our case, the opposite polarization) is much slower than the transition out of that undesired state and into another "measuring" state (in our case an excited absorber state). In such a situation, any growth in the population of the undesired state is quickly lost to the measuring state, ultimately leaving the undesired state at 0 probability.

To this end, we calculate the relevant transition rates for $|R\rangle|G\rangle \rightarrow |L\rangle|G\rangle$ and $|R\rangle|G\rangle \rightarrow |R\rangle|E\rangle$. The first and second order transition probabilities as a function of time are calculated using the formulae [25]

$$P_{i\rightarrow f}(t) = \left|\frac{1}{i\hbar}\int_{t_i}^{t_f} dt' \langle f|\hat{H}_I(t')|i\rangle\right|^2 \tag{11}$$

and

$$P_{i\rightarrow f}(t) = \left|\frac{1}{(i\hbar)^2}\int_{t_i}^{t_f} dt' \int_{t_i}^{t_f} dt'' \sum_m \langle f|\hat{H}_I(t')|m\rangle\langle m|\hat{H}_I(t'')|i\rangle\right|^2. \tag{12}$$

Here, $\hat{H}_I(t)$ is the time-dependent interaction Hamiltonian and i and f denote the initial and final states of the system respectively. The Hamiltonian of our system is given by

$$\hat{H} = \hat{H}_0 + \hat{H}_I \tag{13}$$

where

$$\hat{H}_0 = \hbar\omega(\hat{a}_R^\dagger \hat{a}_R + \hat{a}_L^\dagger \hat{a}_L + 1) + \frac{1}{2}\omega_0 \hat{\sigma}_z \tag{14}$$

is the rest Hamiltonian and

$$\hat{H}_I = \hbar\hat{\Phi} + \hbar\lambda(\hat{a}_L\hat{\sigma}^+ + \hat{a}_L^\dagger\hat{\sigma}^-) \tag{15}$$

is the interaction Hamiltonian. Finally, ω is the frequency of light and ω_0 is the resonant frequency of the two-level atom and these are assumed equal in the calculation. The parameter λ is the coupling between the atom and the light, and σ_z is the Pauli Z spin operator with $\hat{\sigma}^\pm$ the Pauli ladder operators. The phase component of the interaction Hamiltonian, $\hat{\Phi}$, is obtained from eq. (9) and is given by

$$\hat{\Phi} = \begin{bmatrix} \phi_H & 0 \\ 0 & \phi_V \end{bmatrix} \tag{16}$$

in the linear basis. In evaluating (11) and (12), our initial and final states are in terms of circular polarization states, but we perform the calculation in the linear basis, rewriting $\hat{a}_R^\dagger \rightarrow (\hat{a}_H^\dagger - i\hat{a}_V^\dagger)/\sqrt{2}$ and $\hat{a}_R^\dagger \rightarrow (\hat{a}_H^\dagger + i\hat{a}_V^\dagger)/\sqrt{2}$ and their corresponding lowering operators.

With all this, we calculate the first and second order transitions from an initial state $|i\rangle = |R\rangle|G\rangle$, into final states $|f\rangle = |L\rangle|G\rangle$ and $|f\rangle = |0\rangle|E\rangle$. Our time-dependent transition probabilities, $P_{RG\rightarrow LG}$ and $P_{RG\rightarrow 0G}$ are therefore

$$P_{RG\rightarrow LG}(t) = \frac{t^2}{4}(\phi_H - \phi_V)^2 + \frac{t^4}{16}(\phi_H^2 - \phi_V^2)^2 \tag{17}$$

and

$$P_{RG\rightarrow 0E}(t) = \frac{\lambda^2 t^4}{32}(\phi_H - \phi_V)^2. \tag{18}$$

Note that the result in (17) has both a first and second order contribution while that of (18) only has a second order contribution as the first order probability is 0. Similar results can

be obtained for the opposite case (left polarized photon into right polarized and excited state of a right absorber).

Taking the ratio of the probabilities, $P_{\phi/E} = P_{RG\to LG}/P_{RG\to 0E}$, provides some insight into the necessary conditions for the Zeno effect. Conditions under which the ratio is small indicate that the absorption rate is much larger than the transition rate to left circular polarization. The ratio as a function of time is

$$P_{\phi/E}(t) = \frac{8}{\lambda^2 t^2} + \frac{2}{\lambda^2}(\phi_H + \phi_V)^2. \tag{19}$$

As long as the coupling parameter between the absorbing medium and the photon mode, λ, is significantly larger than the sum of the horizontal and vertical phase shift parameters, then the 2nd term disappears. The same cannot be said for the first term, where the inverse dependence on time means that there is always some short time period during which the phase transition is faster than the absorption. Thankfully, this can be mitigated by increasing the coupling parameter and consequently decreasing the time during which PMD may proceed. In physical sense this would be accomplished by either placing the absorbing medium deeper within the evanescent field or by simply increasing the density of the absorbing medium around the field. Either method introduces an effective increase in absorption rate. Even still, the ratio is only large when $t \sim \lambda^-1$ or smaller, after which the ratio declines, meaning that as long as λ is sufficiently large, the time over which the polarization can shift will be quite small, meaning the accumulated probability that the photon will shift in polarization will remain small.

3. Numerical Simulation

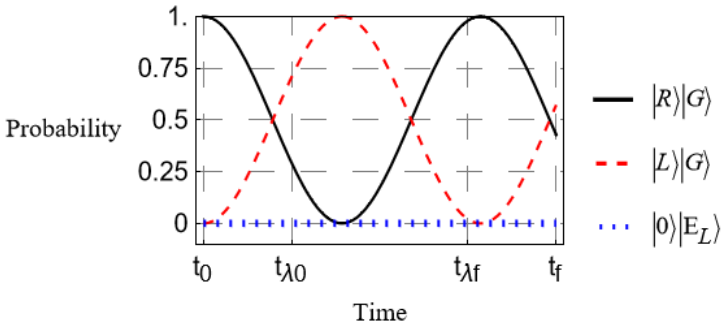

Figure 2. Time-evolution of the polarization state in the approximate form given in Equation (7) as it propagates through a birefringent medium. No absorbers are present. The black curve is the probability that the photon is right polarized, the red dashed curve signifies left polarization, and the blue dotted curve represents the probability of excitation of the absorbers.

In the previous section we looked at the theoretical case of a photon passing through a waveguide of constant birefringence, determined the time-dependence of the polarization, and constructed an approximate time-evolution operator producing PMD. From here we were able to determine an effective time-evolution operator from a Zeno effect, and determine transition probabilities of polarization shift and absorption as a function of time, providing some insight into necessary conditions for a Zeno effect.

In this section, we perform a numerical simulation in Mathematica Documentation of our physical system using the model derived in the previous section. We look at a few relevant cases where we vary the time-dependence of the absorber coupling and the birefringence. Each case is compared with the evolution in absence of absorbers, shown in Figure 2. The time-dependence using the in the short-time regime of Equation (8) is here shown.

The simulation is performed by first constructing the Hamiltonian followed by solving the time-dependent Schrodinger equation [26]

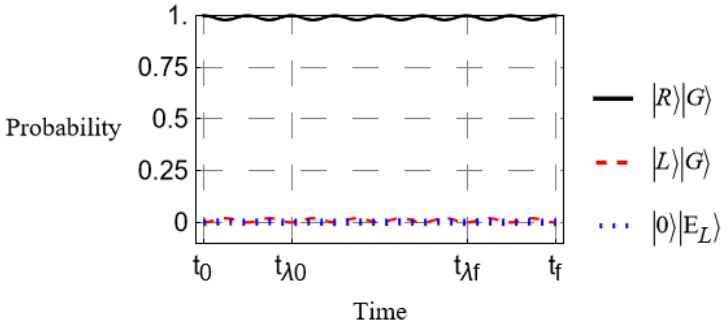

Figure 3. Time-evolution of the polarization state in the presence of absorbers. All curves are labelled as in 2.

$$i\hbar\frac{d|\psi(t)\rangle}{dt} = \hat{H}(t)|\psi(t)\rangle. \tag{20}$$

We assume the intial state is $|\psi(t_0)\rangle = |R\rangle|G\rangle$ and $\hat{H}(t)$ is taken from Eqns. (13), (14), and (15). We further assume an infinite number of absorbers with which the incident photon interacts as it travels through the birefringent medium, therefore the coupling parameters are approximated as a single, continuous potential. In our first case, we examine the case where, as in our theoretical treatment in the last section, the birefringence and coupling to the absorbers is held constan. That is, the ϕ_s do not vary in time, nor does the coupling parameter λ constant. This simplest case is shown in Figure 3.

We see from Figure 2, that absent the absorbers, the polarization shifts cyclically as expected. Comparing with Figure 3, we see that introducing the absorbing medium drastically reduces the probability of transition at any time. Increasing the coupling parameter λ continues this trend to make transitions negligible in probability, as expected, thus realizing total suppression of PMD. As predicted in the previous section, the required coupling strength for effective PMD suppression increases along with the degree of birefringence. In the example of Figure 3, the difference $\phi_H - \phi_V$ is only about 1% off of their average.

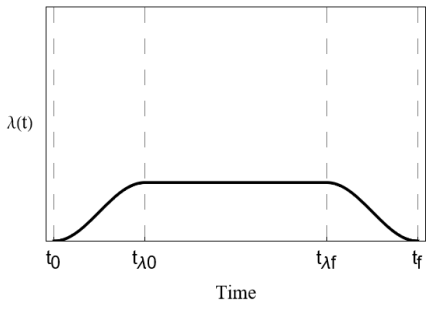

Figure 4. Time-evolution of the coupling parameter $\lambda(t)$ assuming an adiabatic (slowly turned on) potential.

As a matter of interest, we compare an additional scenario. Shown in Figure 5 is a simulation in which we assume an adiabatic approximation, where we slowly turn on the absorber coupling [25]. This case may be somewhat more applicable to a physical implementation of this scheme, as it will generally be the case that PMD will begin to affect an incident photon before it has a chance to interact with any additional absorbing material within the waveguide's path. The time-dependence of $\lambda(t)$ is shown in Figure 4.

We have made the same choice for the coupling parameter in Figure 5 as in Figure 3. Notice that while the probability remains significantly reduced, it is not nearly so good as in Figure 3. Increasing the coupling reduces this just as in the other case, but it requires much stronger coupling to reach similar suppression. Furthermore, the adiabatic "turn off" of the coupling can lead to inconsistent outcomes. See Figure 6 for a comparison

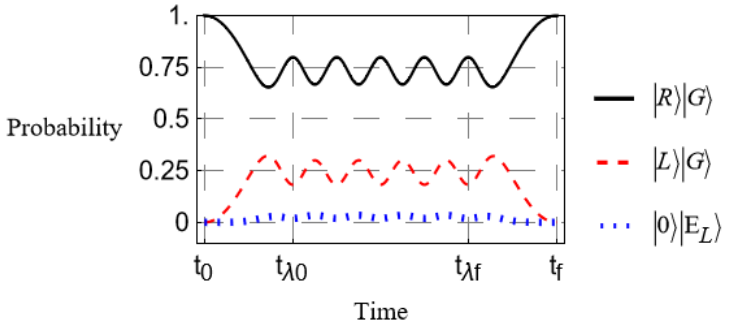

Figure 5. Time-evolution under an adiabatic approximation. The coupling parameter λ is slowly turned on until it reaches a maximum at time $t_{\lambda 0}$ and is slowly turned off at time $t_{\lambda f}$.

between two somewhat different lengths of time over which the coupling parameter is at a maximum. The coupling parameter here is 5 times larger than in the previous examples, so suppression is fairly strong overall, but simply shortening the maximum coupling time $t_f - t_0$ by an arbitrary choice of 10% (5% in the total time of the simulation), yields a much smaller probability that the photon exits in a left polarized state. The case of Figure 5 ending in a nearly perfect right polarized state is nothing more than a happy coincidence. It is uncertain what exactly the minimum transition rate can be for any given coupling parameter, "turn on" rate, etc. though in the case of Figure 6 we found probabilities as low as 59.6% of remaining in the right polarized state.

This is due to the significant transition rate in the short time regime, as expected from the analysis of Equation (19). This doesn't, however, necessarily pose an issue if the coupling is suddenly "turned off", as would be the case when the photon exits the waveguide for instance. Whether this would introduce an quantum decoherence from which-path information [27] is as of yet unclear. Ultimately, this suggests that for implementations of this design, it is of great importance that the incident photon experience strong interaction with the absorbing medium quite early else the output will become much harder to control.

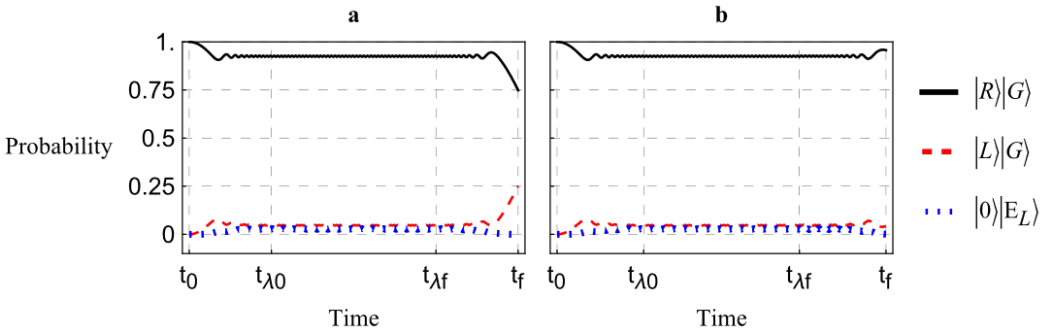

Figure 6. Time-evolution under the assumption that the coupling parameter λ is turned on slowly. λ is chosen to be especially strong for significant suppression of PMD. Both plots are the same, but in a), $t_{\lambda f} - t_{\lambda 0}$ is arbitrarily larger than that same period in b).

These numerical simulations demonstrate, as a proof of concept, that the Zeno effect can be used to suppress polarization mode dispersion under appropriate conditions.

This section may be divided by subheadings. It should provide a concise and precise description of the experimental results, their interpretation as well as the experimental conclusions that can be drawn.

4. Conclusion

Our investigation here demonstrates that the quantum Zeno effect is a promising method for suppressing PMD in optical and quantum communications. This method

avoids the probabilistic, and consequently scalability, issues with cluster states and error correcting codes [12–14] and allows preservation of arbitrary polarization states. This last advantage, however, does require that the state is split into two separate waveguides as the technique will absorb one or the other circular polarization state as it passes through one waveguide since one of the two will be absorbed. Any quantum communications protocols, therefore, will necessarily require dual-rail encodings.

Though other methods can promise similar results in absence of atmospheric effects and temperature fluctuations, such environmental effects on the waveguides can also be mitigated with this proposed Zeno effect. In principle, such a technique would further avoid leaking which-path information to an environment, so that quantum coherence of entanglement is not destroyed. This is a problem in typical fiber communications in no small part due to the fact that the unknown, stochastic nature of birefringence in normal fibers, and in polarization maintaining fibers experiencing atmospheric effects, causing the information to be rendered unusable for quantum protocols [11]. The technique described here would bypass these issues in either situation, though is limited by the extent to which the phase shift in Equation (10) can be made equal. In a physical scenario, the absorbers of right-polarized photons may not be the same type, nor capable of reaching the same coupling or density as the absorbers of left-polarized photons. This could lead to somewhat different phase shifts through the fiber medium, and could affect the entanglement quality. Even so, the phase shifts should be brought close enough together should extend the range over which entangled photons can be transmitted, most particularly if applied in regions of significant PMD.

In addition, the technique has potential for applications of nonlocal dispersion cancellation [22,23], conditioned on proper engineering of the refractive indices. Indeed, nonlocal cancellation of dispersion may be simply combined with this technique to further improve the transmission rates of entangled photons.

In this investigation, we have demonstrated both analytically and numerically that a quantum Zeno effect can be employed in birefringent media to suppress PMD. The limitations on the effectiveness of the method are primarily related to how quickly the Zeno effect can be applied before significant PMD affects the photon, the coupling strength itself, and the rate at which the birefringence changes along the length of the waveguide. It should be particularly useful in protecting fragile quantum information encoded in the polarization degree of freedom as it travels through waveguides experiencing significant atmospheric effects, and overall reduce the need for quantum repeating protocols for long distance communications.

Author Contributions: Investigation, Ian C. Nodurft; Formal Analysis, Ian C. Nodurft; Software, Ian C. Nodurft; Writing - Original Draft, Ian C. Nodurft; Validation, Alejandro Rodriguez Perez; Writing - Review and Editing, Alejandro Rodriguez Perez and Harry C. Shaw; Supervision, Harry C. Shaw; Funding Acquisition, Harry C. Shaw. All authors have read and agreed to the published version of the manuscript.

For research articles with several authors, a short paragraph specifying their individual contributions must be provided. The following statements should be used "Conceptualization, X.X. and Y.Y.; methodology, X.X.; software, X.X.; validation, X.X., Y.Y. and Z.Z.; formal analysis, X.X.; investigation, X.X.; resources, X.X.; data curation, X.X.; writing—original draft preparation, X.X.; writing—review and editing, X.X.; visualization, X.X.; supervision, X.X.; project administration, X.X.; funding acquisition, Y.Y. All authors have read and agreed to the published version of the manuscript.", please turn to the CRediT taxonomy for the term explanation. Authorship must be limited to those who have contributed substantially to the work reported.

Funding: This research was funded under NASA SENSE contract 80GSFC19C0063 to Peraton.

Institutional Review Board Statement: Not applicable

Informed Consent Statement: Not applicable

Data Availability Statement: No new data were created or analyzed in this study. Data sharing is not applicable to this article.

Acknowledgments:

Conflicts of Interest: The authors declare no conflicts of interest.

Abbreviations

The following abbreviations are used in this manuscript:

MDPI	Multidisciplinary Digital Publishing Institute
DOAJ	Directory of open access journals
TLA	Three letter acronym
LD	Linear dichroism

Appendix A

Appendix A.1 Time-dependent Polarization

We assume a single-photon enters a birefringent medium, such as an optical fiber, after passing through a narrow bandwidth filter. The general single-photon state is [22,23]

$$|\psi(0)\rangle = c_N \int d\omega g(\omega) \hat{a}^\dagger_{k,s} |0\rangle \tag{A1}$$

where $g(\omega)$ is approximated by a Gaussian centered on frequency ω_F due to passing through the narrow bandwidth filter. The constant c_N is a suitable normalization constant, and the subscripts k and s refer to the wavenumber and polarizations respectively. To obtain the time-dependence of the polarization, we apply the electric field operator in one dimension [24]

$$\hat{\mathbf{E}}(x,t) = i \sum_{k,s} \sqrt{\frac{2\pi\hbar\omega_k}{V}} \hat{\mathbf{e}}_{k,s} \hat{a}^\dagger_{k,s} e^{i(kx-\omega_k t)}. \tag{A2}$$

Transforming Equation (A1) into integral form, then applying it to Equation (A2), and further replacing $g(\omega) \to \exp\left[-(\omega-\omega_F)^2/\sigma_F^2\right]$ due to applying the filter we obtain the time-dependent state

$$|\psi(t)\rangle = c'_N \int d\omega \sqrt{\omega} e^{\frac{-(\omega-\omega_F)^2}{\sigma_F^2}} e^{-i\omega t} [e^{ik_H x_H}|H\rangle - ie^{ik_V x_V}|V\rangle]. \tag{A3}$$

We have assumed the photon begins in the polarization state $|R\rangle = (|H\rangle - i|V\rangle)/\sqrt{2}$. Noting the narrow bandwidth, we can approximate the slowly varying $\sqrt{\omega}$ as a constant equal to the filter center frequency $\sqrt{\omega_F}$. The wavenumber is replaced according to which polarization state $\hat{\mathbf{E}}$ is applied by the expanded form

$$k_s = k_{0,s} + \alpha_s(\omega - \omega_F) + \beta_s(\omega - \omega_F)^2 \tag{A4}$$

and the frequency under the integral is replaced by

$$\omega_k = \omega_F + \epsilon. \tag{A5}$$

With these replacements, the integral becomes

$$|\psi(t)\rangle = c'_N \int d\epsilon e^{-\frac{\epsilon^2}{\sigma_F^2}} e^{-i\epsilon t} [e^{i(\alpha_H\epsilon+\beta_H\epsilon^2)x_H}|H\rangle - ie^{i(\alpha_V\epsilon+\beta_V\epsilon^2)x_V}|V\rangle]. \tag{A6}$$

The factors independent of ϵ have all been absorbed into the normalization constant. Following the identity

$$\int_{-\infty}^{\infty} dx e^{-(ax^2+bx+c)} = \sqrt{\frac{\pi}{a}} e^{(b^2-4ac)/4a} \tag{A7}$$

we evaluate the integral and obtain

$$|\psi(t)\rangle = c_N''\Big(\frac{e^{\frac{(\alpha_H x_H - t)^2}{4(-\frac{1}{2\sigma_F^2}+i\beta_H x_H)}}}{\sqrt{-\frac{1}{2\sigma_F^2}+i\beta_H x_H}}|H\rangle - i\frac{e^{\frac{(\alpha_V x_V - t)^2}{4(-\frac{1}{2\sigma_F^2}+i\beta_V x_V)}}}{\sqrt{-\frac{1}{2\sigma_F^2}+i\beta_V x_V}}|V\rangle\Big). \tag{A8}$$

Making the replacement $x_s \to v_s t = ct/n_s$, and converting complex numbers into polar form, we obtain

$$|\psi(t)\rangle = c_N''\Big(\sqrt{\frac{\gamma_H}{\mu_H}}e^{\frac{\kappa_H^2\gamma_H t^2}{4\mu_H}}|H\rangle - i\sqrt{\frac{\gamma_V}{\mu_V}}e^{\frac{\kappa_V^2\gamma_V t^2}{4\mu_H}}|V\rangle\Big). \tag{A9}$$

where

$$\begin{aligned}\kappa_s &= (\frac{\alpha_s}{n_s}c - 1),\\ \mu_s &= \sqrt{\frac{1}{4\sigma_F^4}+\frac{\beta_H^2}{n_H^2}c^2t^2},\\ \gamma_s &= e^{i\arctan 2\sigma_F^2\frac{\beta_H}{n_H}ct}.\end{aligned} \tag{A10}$$

By taking $t \to 0$, these parameters can be simplified to $\mu_s \to 1/2\sigma_F^2$ and $\gamma_s \to exp(2i\sigma_F^2\beta_s^2c^2t^2)$. Collecting all the time-dependence in the exponents, and dropping all second-order and higher terms in t yields the result $\phi_s \approx \sigma_F^2 c\beta_s^2/n_s^2$ shown in Equation (8). Taking $t \to \infty$ instead simplifies the parameters $\mu_s \to \beta_s ct/n_s$ and $\gamma_s \to exp(i\pi/2) = i$. Cancelling a factor of t from the numerator and denominator of the exponents gives the alternate result from Equation (8), $\phi_s \approx n_s/(4\beta_s c)(\alpha_s/n_s - 1)^2$. Thus we derive our approximate form of the normalized polarization time-evolution:

$$|\psi(t)\rangle \approx \frac{1}{\sqrt{2}}\Big(e^{-i\phi_H t}|H\rangle - ie^{-i\phi_V t}|V\rangle\Big). \tag{A11}$$

Appendix A.2 Quantum Zeno Dynamics

The quantum Zeno effect relies on making frequent measurements with very small time in between to suppress the quantum state evolution in some desirable way [15,16]. We begin by looking at an arbitrary quantum system in a quantum state described by the density matrix $\hat{\rho}_0$, which evolves according to time-evolution operator $\hat{U}(t) = exp(-i\hat{H}t)$, where $\hat{H}$ is a time-independent Hamiltonian. Measurements are denoted by the projection operator $\hat{E}$ into some subspace $\boldsymbol{H}_E$ of the total Hilbert space $\boldsymbol{H}$. ρ_0 is assumed to belong to $\boldsymbol{H}_E$. The density matrix at some time T is found by

$$\hat{\rho}(T) = \hat{U}(T)\hat{\rho}_0\hat{U}^\dagger(T). \tag{A12}$$

The probability of the quantum state remaining in $\boldsymbol{H}_E$ is

$$P(T) = Tr[\hat{E}\hat{U}(T)\hat{\rho}_0\hat{U}^\dagger(T)\hat{E}]. \tag{A13}$$

We note that $\hat{\rho}_0 = \hat{E}\hat{\rho}_0\hat{E}$. After evolution for time t and projection, the state is

$$\begin{aligned}\hat{\rho}(t) &= \hat{E}\hat{U}(t)\hat{\rho}_0\hat{U}^\dagger(t)\hat{E}.\\ &= \hat{E}\hat{U}(t)\hat{E}\hat{\rho}_0\hat{E}\hat{U}^\dagger(t)\hat{E}\\ &= \hat{v}(t)\hat{\rho}_0\hat{v}^\dagger(t)\end{aligned} \tag{A14}$$

where $\hat{v}(t) = \hat{E}\hat{U}(t)\hat{E}$ is an effective, nonunitary in $\boldsymbol{H}$ time-evolution operator. Performing N measurements over total time T, the state evolves as

$$\hat{\rho}^{(N)}(T) = [\hat{v}(T/N)]^N \hat{\rho}_0 [\hat{v}^\dagger(T/N)]^N. \tag{A15}$$

If we take the limit $N \to \infty$ we can obtain the effective time-evolution operator $\hat{V}(T)$ for an ideal Zeno effect from continuous measurement.

The system in question involves an incident right-circularly polarized photon, entering a birefringent medium, and the destruction of left-circularly polarized photons serves to project the polarization state back to right-circular. The various terms are, therefore,

$$\begin{aligned} \hat{\rho}_0 &= |R\rangle\langle R|, \\ \hat{E} &= |R\rangle\langle R|, \\ \hat{U}(t) &= \begin{bmatrix} e^{-i\phi_H t} & 0 \\ 0 & e^{-i\phi_V t} \end{bmatrix}. \end{aligned} \tag{A16}$$

Taking $\hat{E}$ and $\hat{U}(t)$ into matrix form, we evaluate $\hat{v}(t)$ as

$$\begin{aligned} \hat{v}(t) &= \hat{E}\hat{U}(t)\hat{E} \\ &= \frac{1}{\sqrt{2}^4} \begin{bmatrix} 1 & i \\ -i & 1 \end{bmatrix} \begin{bmatrix} e^{-i\phi_H t} & 0 \\ 0 & e^{-i\phi_V t} \end{bmatrix} \begin{bmatrix} 1 & i \\ -i & 1 \end{bmatrix} \\ &= \frac{1}{4} \begin{bmatrix} (e^{-i\phi_H t} + e^{-i\phi_V t}) & i(e^{-i\phi_H t} + e^{-i\phi_V t}) \\ -i(e^{-i\phi_H t} + e^{-i\phi_V t}) & (e^{-i\phi_H t} + e^{-i\phi_V t}) \end{bmatrix} \\ &= \frac{1}{4}(e^{-i\phi_H t} + e^{-i\phi_V t}) \begin{bmatrix} 1 & i \\ -i & 1 \end{bmatrix} \\ &= \frac{1}{2}(e^{-i\phi_H t} + e^{-i\phi_V t})|R\rangle\langle R|. \end{aligned} \tag{A17}$$

Taking $\hat{v}(t)$ to the Nth power, and replacing $t \to T/N$ we obtain

$$\begin{aligned} \hat{v}^N\Big(\frac{T}{N}\Big) &= \frac{1}{2^N}(e^{-i\phi_H \frac{T}{N}} + e^{-i\phi_V \frac{T}{N}})^N (|R\rangle\langle R|)^N \\ &= \frac{1}{2^N}(e^{-i\phi_H \frac{T}{N}} + e^{-i\phi_V \frac{T}{N}})^N |R\rangle\langle R|. \end{aligned} \tag{A18}$$

For a continuous Zeno effect, we will take the limit $N \to \infty$. However, we'll first transform the complex exponential sum in Equation (A18) into polar form, and distributing the factor of $1/2$ into the result.

$$\begin{aligned} \frac{1}{2}(e^{-i\phi_H \frac{T}{N}} + e^{-i\phi_V \frac{T}{N}}) &= \frac{1}{2}\sqrt{2 + 2\cos\Big[(\phi_H - \phi_V)\frac{T}{N}\Big]}\, e^{i \arctan\left[\xi(\frac{T}{N})\right]} \\ &= \sqrt{\frac{1 + 1\cos\Big[(\phi_H - \phi_V)\frac{T}{N}\Big]}{2}}\, e^{i \arctan\left[\xi(\frac{T}{N})\right]} \\ &= \Big|\cos\Big[(\phi_H - \phi_V)\frac{T}{2N}\Big]\Big| e^{i \arctan\left[\xi(\frac{T}{N})\right]}. \end{aligned} \tag{A19}$$

Here we have taken advantage of the identity $\cos\theta^2 = (1 + \cos\theta)/2$ to simplify the magnitude. The function $\xi(T/N)$ is

$$\xi\Big(\frac{T}{N}\Big) = \frac{\sin(\phi_H \frac{T}{N}) + \sin(\phi_V \frac{T}{N})}{\cos(\phi_H \frac{T}{N}) + \cos(\phi_V \frac{T}{N})}. \tag{A20}$$

We now have the limit

$$\begin{aligned}\lim_{N\to\infty}\hat{v}^N\Big(\frac{T}{N}\Big) &= \lim_{N\to\infty}\Big|\cos\Big[(\phi_H-\phi_V)\frac{T}{2N}\Big]\Big|^N e^{Ni\arctan\left[\xi(\frac{T}{N})\right]}\\ &= \lim_{N\to\infty}\Big|\cos\Big[(\phi_H-\phi_V)\frac{T}{2N}\Big]\Big|^N \lim_{N\to\infty} e^{Ni\arctan\left[\xi(\frac{T}{N})\right]}.\end{aligned} \tag{A21}$$

We can tackle each element of the limit separately, though they will both use similar techniques. In both cases, we'll start by setting the argument equal to y and taking $\ln y$, followed by the use of L'Hopital's Rule. We start by evaluating limit of the magnitude factor.

$$\begin{aligned}\lim_{N\to\infty}\ln y &= \lim_{N\to\infty} N\ln\Big|\cos\Big[(\phi_H-\phi_V)\frac{T}{2N}\Big]\Big|\\ &= \lim_{N\to\infty}\frac{\ln\Big|\cos\Big[(\phi_H-\phi_V)\frac{T}{2N}\Big]}{1/N}.\end{aligned} \tag{A22}$$

Applying L'Hopital's Rule we get

$$\begin{aligned}\lim_{N\to\infty}\ln y &= \lim_{N\to\infty}\frac{\sin\Big[(\phi_H-\phi_V)\frac{T}{2N}\Big]\mathrm{sgn}\Big[\cos\Big[(\phi_H-\phi_V)\frac{T}{2N}\Big]\Big](\phi_H-\phi_V)\frac{T}{2}(-1/N^2)}{-1/N^2\Big|\cos\Big[(\phi_H-\phi_V)\frac{T}{2N}\Big]\Big|}\\ &= \lim_{N\to\infty}\frac{\sin\Big[(\phi_H-\phi_V)\frac{T}{2N}\Big]\mathrm{sgn}\Big[\cos\Big[(\phi_H-\phi_V)\frac{T}{2N}\Big]\Big](\phi_H-\phi_V)\frac{T}{2}}{\Big|\cos\Big[(\phi_H-\phi_V)\frac{T}{2N}\Big]\Big|}.\end{aligned} \tag{A23}$$

The "sign" function sgn(x) returns 1 if x is positive, -1 if x is negative, and 0 if x is 0. Note that $\lim_{N\to\infty} 1/N = \lim_{x\to 0^+} x$ since N is approaching positive ∞. The components of the limit are, then each evaluated to be

$$\begin{aligned}&\lim_{N\to\infty}\sin\Big[(\phi_H-\phi_V)\frac{T}{2N}\Big] = 0\\ &\lim_{N\to\infty}\mathrm{sgn}\Big[\cos\Big[(\phi_H-\phi_V)\frac{T}{2N}\Big]\Big] = 1\\ &\lim_{N\to\infty}\Big|\cos\Big[(\phi_H-\phi_V)\frac{T}{2N}\Big]\Big| = 1.\end{aligned} \tag{A24}$$

Thus, the limit is evaluated as

$$\begin{aligned}&\lim_{N\to\infty}\ln y = 0\\ \implies &\lim_{N\to\infty} y = 1.\end{aligned} \tag{A25}$$

Following a similar process, we evaluate the limit of the complex exponential term. Due to the complexity of the calculation, we will first note the derivative of our term $\xi(T/N)$ with respect to N.

$$\frac{d\xi}{dN} = -\frac{T(\phi_H+\phi_V)}{N^2}\frac{1+\cos\Big[(\phi_H-\phi_V)\frac{T}{N}\Big]}{\Big[\cos\Big(\phi_H\frac{T}{N}\Big)+\cos\Big(\phi_V\frac{T}{N}\Big)\Big]^2}. \tag{A26}$$

Our new limit is

$$\begin{aligned}\lim_{N\to\infty} \ln y &= \lim_{N\to\infty} Ni \arctan\left[\xi\left(\frac{T}{N}\right)\right] \\ &= i \lim_{N\to\infty} \frac{\arctan\left[\xi\left(\frac{T}{N}\right)\right]}{1/N}\end{aligned} \tag{A27}$$

and again using L'Hopital's Rule we get

$$\begin{aligned}\lim_{N\to\infty} \ln y &= i \lim_{N\to\infty} \frac{T(-1/N^2)(\phi_H+\phi_V)\left[1+\cos\left[(\phi_H-\phi_V)\frac{T}{N}\right]\right]}{(-1/N^2)\left[1+\xi^2\left(\frac{T}{N}\right)\right]\left[\cos\left(\phi_H\frac{T}{N}\right)+\cos\left(\phi_V\frac{T}{N}\right)\right]^2} \\ &= i(\phi_H+\phi_V)T \lim_{N\to\infty} \frac{\left[1+\cos\left[(\phi_H-\phi_V)\frac{T}{N}\right]\right]}{\left[1+\xi^2\left(\frac{T}{N}\right)\right]\left[\cos\left(\phi_H\frac{T}{N}\right)+\cos\left(\phi_V\frac{T}{N}\right)\right]^2}.\end{aligned} \tag{A28}$$

Looking at the various pieces of the limit, we see that

$$\begin{aligned}&\lim_{N\to\infty} \xi\left(\frac{T}{N}\right) = 0 \\ &\lim_{N\to\infty} \cos\left(\phi_s\frac{T}{N}\right) = 1 \\ &\lim_{N\to\infty} \cos\left[(\phi_H-\phi_V)\frac{T}{N}\right] = 1.\end{aligned} \tag{A29}$$

The subscript s refers to either H and V. Therefore, the limit evaluates to

$$\begin{aligned}&\lim_{N\to\infty} \ln y = \frac{i}{2}(\phi_H+\phi_V)T \\ \implies &\lim_{N\to\infty} y = e^{\frac{i}{2}(\phi_H+\phi_V)T}.\end{aligned} \tag{A30}$$

Thus, the effective time-evolution operator in the limiting case of continuous observation is

$$\begin{aligned}\hat{V}(T) &\equiv \lim_{N\to\infty} \hat{v}^N\left(\frac{T}{N}\right) \\ &= e^{\frac{i}{2}(\phi_H+\phi_V)T}|R\rangle\langle R|.\end{aligned} \tag{A31}$$

References

1. Govind P. Agrawal; *Nonlinear Fiber Optics*, 6th ed.; Academic Press, 525 B Street, Suite 1650, San Diego, CA92101, United States, 2019; pp. 11-14, 236-240, 443-446
2. herwig Kogelnik; Robert M. Jopsonm Lynn E. Nelson, *Optical Fiber Telecommunications IV-B*, 4th ed.; Academic Press, 2002; pp. 725-861
3. Katsunari Okamoto; *Fundamentals of Optical Waveguides*, 2nd ed.; Academic Press, 2006; pp. 57-158
4. N. Gisin, J.-P. Von der Weid, and J.-P. Pellaux; Polarization mode dispersion of short and long single-mode fibers. *J. Lightwave Technol.*, **1991**, *9*, 821-827
5. J. Noda, K. Okamoto, Y. Sasaki; Polarization-maintaining fibers and their applications. *J. Lightwave Technol.* **1986**, *4*, 1071-1089
6. D.N. Payne, A.J. Barlow, and J.J.R. Hansen; Development of Low- and High- Birefringence Optical Fibers. *IEEE J. Quantum Electron.* **1982**; 477
7. S.C. Rashleigh; Origins and control of polarization effects in single-mode fibers. *J. Lightwave Technol.* **1983**; 312
8. K. Tajima, M. Ohashi, and Y. Sasaki; A new single-polarization optical fiber. *J. Lightwave Technol.* **1989**; 1499
9. M.J. Messerly, J.R. Onstott, and R.C. Mikkelson; A Broad-Band Single Polarization Optical Fiber. *J. Lightwave Technol.* **1991**; 817

10. R.B. Dyott; *Elliptical Fiber Waveguides*, Artec House, 1995
11. J. Dubovan, J. Litvik, D. Benedikovic, J. Mullerov, I. Glesk, A. Veselovsky, and M. Dado; Impact of Wind Gust on High-Speed Characteristics of Polarization Mode Dispersion in Optical Power Ground Wire Cables. *Sensors.* **2020**;
12. R. Raussdorf and H. J. Briegel; A One-Way Quantum Computer. *Phys. Rev. Lett.* **2001**; 5188-5191
13. R. Raussendorf, D. E. Browne, and H. J. Briegel; Measurement-based quantum computation on cluster states. *Phys. Rev. A.* **2003**; 022312
14. M. A. Nielsen; I. L. Chuang. *Quantum Computation and Quantum Information*, 1st ed.; Cambridge University Press: University Printing House, Cambridge CB2 8BS, United Kingdom, 2010; pp. 425-499
15. B. Misra and E. C. G. Sudarshan; The Zeno's paradox in quantum theory. *J. Math. Phys.* **1977**; 756-763
16. P. Facchi, V. Gorini, G. Marmo, S. Pascazio, E. C. G. Sudarshan; Quantum Zeno Dynamics. *Phys. Lett. A.* **2000**; 12-19
17. F. Schafer, I. Herrera, S. Cherukattil, C. Lovecchio, F.S. Cataliotti, F. Caruso, A. Smerzi; Experimental realization of quantum zeno dynamics. *Nat. Commun.* **2014**;
18. J. D. Franson, B. C. Jacobs, T. B. Pittman; Quantum computing using single photons and the Zeno effect. *Phys. Rev. A.* **2004**; 062302
19. N. ten Brinke, A. Osterloh, R. Schutzhold; Entangling photons via the double quantum Zeno effect. *Phys. Rev. A.* **2011**; 022317
20. S. U. Shringarpure, J. D. Franson; Inhibiting Phase Drift in Multi-Atom Clocks Using the Quantum Zeno Effect. *Frontiers in Optics + Laser Science 2022 (FIO, LS).* **2022**;
21. I. C. Nodurft, H. C. Shaw, R. T. Glasser, B. T. Kirby, T. A. Searles; Generation of polarization entanglement via the quantum Zeno effect. *Opt. Express.* **2022**; 31971-31985
22. Franson, J. D.; Nonlocal cancellation of dispersion. *Phys. Rev. A.* **1992**; 3126-3132
23. I. C. Nodurft, S. U. Shringarpure, B. T. Kirby, T. B. Pittman, J. D. Franson; Nonlocal dispersion cancellation for three or more photons. *Phys. Rev. A.* **2020**; 013713
24. Gerry, C. C., Knight, P. L.; *Introductory Quantum Optics*; Cambridge University Press: The Edinburgh Building, Cambridge CB2 8RU, UK; pp. 23
25. Baym, G.; *Lectures on Quantum Mechanics*; Addison-Wesley Publishing Company, Inc: 350 Bridge Parkway, Redwood City, California, 1969; pp. 246-258
26. Cohen-Tannoudji, C., Diu, B., Laloe, F.; *Quantum Mechanics*; Hermann and John Wiley I& Sons. Inc.: Paris, France; pp. 222
27. M. O. Scully, K. Druhl; Quantum eraser: A proposed photon correlation experiment concerning observation and "delayed choice" in quantum mechanics. *Phys. Rev. A.* **1982**; 2208-2213